Intrinsic Sorptivity and Water Infiltration into Dry Soil at Different Degrees of Saturation

K. E. Schulte[1], P. J. Culligan[2] and J. T. Germaine[3]

[1]ASCE Student Member, Department of Civil Engineering and Engineering Mechanics, Columbia University, New York, NY 10027, Email: kes2115@columbia.edu
[2]ASCE Member, Department of Civil Engineering and Engineering Mechanics, Columbia University, New York, NY 10027, Email: pjc2104@columbia.edu
[3]ASCE Member, Department of Civil and Environmental Engineering, Massachusetts Institute of Technology, Cambridge, MA 02139, Email: jgermain@mit.edu

Key words: Infiltration, Sorptivity, Vadoze Zone, Unsaturated transport

Abstract: The sorptivity S quantifies the effect of capillarity on liquid movement in a porous material. For liquid infiltration into an initially dry material, S is a parameter that is contingent on both liquid and material properties as well as the maximum liquid content behind the infiltrating front, θ_m. In prior work, Culligan et al. (2005) used scaling analyses to derive a dimensionless, intrinsic sorptivity S^* that is constant for different liquids, Miller-similar materials and differing values of $S_{e(av)}$., the average degree of saturation behind the infiltrating front. The validity of the dimensionless S^*, and an accompanying dimensionless Boltzmann transformation Φ^*, was tested for different liquids by examining the horizontal infiltration profiles of water and Soltrol 220 in uniform dry sand at a constant $S_{e(av)} = 0.79$. This work extends the validity testing of S^* and Φ^* to conditions of varying $S_{e(av)}$. Twenty-one distilled water horizontal infiltration experiments, with a range $0.64 \bullet S_{e(av)} \bullet 0.86$, were preformed in uniform dry sand packed at an average porosity $n = 0.36$. The results of the tests indicate an intrinsic sorptivity value of 0.121, which compares well with the value of $S_{av}^* = 0.128$ reported by Culligan et al. The work also confirms that the dimensionless Boltzmann transformation Φ^* can be used to generate a similarity profile for moisture content, even when infiltration takes place under different degrees of saturation.

1. Introduction

The process by which a wetting liquid displaces air in a porous material, usually termed liquid infiltration, has been the subject of study for over a century [Slichter (1898), Green et al. (1911), Neilson et al. (1962)]. In soils, understanding liquid infiltration is important for predicting unsaturated flow and transport through the vadoze zone and/or partially saturated soil barriers such as landfill caps. There have been many models developed to describe liquid infiltration in a porous material [e.g., Barry (1995), Parlange (1982)]. In general, these models predict the time-rate of infiltration and the cumulative volume of infiltration based on parameters like the sorptivity S [Tindall (1999)], which quantifies the effect of capillarity on a liquid's movement in a material.

Considering horizontal flow, where gravitational forces in the direction of the movement can be neglected, best isolates the effect of capillarity on liquid movement in an unsaturated material. Horizontal one-dimensional flow of a liquid in a rigid, stationary porous material may be described by a non-linear diffusion equation, often referred to as Richard's equation [Tindall (1999)]

$$\frac{\partial\theta}{\partial t}=\frac{\partial}{\partial x}\left(D(\theta)\frac{\partial\theta}{\partial x}\right), \tag{1}$$

where θ is the average volumetric liquid content of the infiltrating fluid, $D(\theta)$ is the hydraulic diffusivity, t is the time and x the spatial coordinate.

The hydraulic diffusivity is a non-linear function of liquid content given by

$$D(\theta)=K(\theta)\frac{\partial h}{\partial\theta}, \tag{2}$$

where K is the hydraulic conductivity of the material at liquid content θ and h is the liquid pressure head at the same liquid content.

To obtain Eq. (1) in the form of an ordinary differential equation, the Boltzmann transformation, $\Phi = xt^{-1/2}$ is used, leading to the solution

$$x(\theta,t)=\Phi(\theta)t^{1/2}, \tag{3}$$

for the boundary conditions $\theta = \theta_i$ at $\Phi = \bullet$ and $\theta = \theta_m$ at $\Phi = 0$, which were satisfied for the experiments reported here.

For liquid infiltration into a porous material that is initially dry (i.e., $\theta_i = 0$), the volume of liquid infiltration per unit area is thus

$$i(t)=t^{1/2}\int_0^{\theta_m}\Phi d\theta. \tag{4}$$

By definition $\int_0^{\theta_m}\Phi d\theta$ is the sorptivity S of the material [Lockington et al (1999)]. S can be determined from observations of liquid infiltration with time into a porous material. S is related to $D(\theta)$ by

$$S=-2D(\theta_m)\frac{d\theta_m}{d\Phi}. \tag{5}$$

Hence, from Eq. (2)

$$S=-2K(\theta_m)\frac{dh_m}{d\left(x/t^{1/2}\right)}. \tag{6}$$

By inspection of Eq. (6), S is a function of the parameters controlling; (i) the hydraulic conductivity of the porous system, namely the grain size distribution and porosity, n, of the porous material, the viscosity, μ, and density, ρ, of the infiltrating liquid, and the relative permeability, k_r, of the infiltrating liquid at $\theta = \theta_m$, and (ii) the liquid pressure head at the inlet to the porous medium, which will depend upon the surface tension, σ, of the infiltrating liquid, its contact angle, ϕ, the density, ρ, of the infiltrating liquid and the average radius, r, of the liquid-air interface within the porous medium at $\theta = \theta_m$.

Culligan et al. (2005) applied the principles of Miller-scaling [Miller (1980)] to derive an intrinsic sorptivity, S^*, that is independent of the porous medium and infiltrating liquid properties noted above, and is given by

$$S^*=\left(\frac{\mu S_{e_m}^c}{l\beta\sigma\theta_m}\right)^{1/2}S, \tag{7}$$

where l is a microscopic characteristic length of the medium, $S_{e(m)} = \theta_m/n$, the average saturation of the infiltrating fluid at the inlet to the porous medium, and $\beta = \cos\phi$. In deriving Eq. (7) is was assumed that k, the intrinsic permeability of the porous medium, is approximated by $k = l^2$, $k_r = S_e^b$ and $r = l\,S_e^a$ [Smith et al. (1978)]. Note, $c = a - b$.

Theoretically, S^* will be a constant for all porous systems with Miller-similar materials, in other words, porous media that are geometrically similar.

Culligan et al. (2005) also applied the principles of Miller-scaling to derive a general, dimensionless Boltzmann variable, namely

$$\Phi^* = \left(\frac{\mu \theta_m S_{e_m}^c}{l \beta \sigma} \right)^{1/2} \Phi . \tag{8}$$

Profiles of Φ^* versus $\theta^*(x\ t)$ should match for Miller-similar materials, where, for initially dry media,

$$\theta^*(x,t) = \frac{\theta(x,t)}{\theta_m} . \tag{9}$$

Calculation of S^* and Φ^* requires knowledge of θ_m, the liquid content at the inlet of the porous medium. Because quantification of θ_m usually requires destructive sampling of a porous medium at the end of an infiltration event, Culligan et al. (2005) proposed re-writing Eqs. (7) and (8) in terms of in terms of $\theta_{av} = i(t)/x(t)$ and $S_{e(av)} = \theta_{av}/n$. The advantage of this approach is that θ_{av} can be obtained from non-destructive observations that are made during an infiltration test. Re-writing Eq. (7) and Eq. (8) in terms of θ_{av} and $S_{e(av)}$ gives

$$S_{av}^* = \left(\frac{\mu S_{e_{av}}^{(c-1)}}{l \beta \sigma n} \right)^{1/2} S , \tag{10}$$

and

$$\Phi_{av}^* = \left(\frac{\mu n S_{e_{av}}^{(c+1)}}{l \beta \sigma} \right)^{1/2} \Phi \tag{11}$$

where the subscript (av) is used to clarify that a dimensionless variable has been defined using θ_{av} and $S_{e(av)}$.

Culligan et al. (2005) investigated the validity of the proposed S_{av}^* and Φ_{av}^* by examining the infiltration of both water and Soltrol 220 into uniform dry sand packed at an average porosity $n = 0.38$. These infiltration experiments indicated an average value of $S_{av}^* = 0.128$. Although Culligan et al. (2005) performed their tests over a range of θ_{av} and $S_{e(av)}$ values, they only conducted destructive evaluation of samples for tests performed at an average $S_{e(av)} = 0.79$. Hence, they were only able to investigate the validity of Φ_{av}^* for a constant $S_{e(av)}$. To further investigate if the dimensionless Boltzmann variable holds true over a range of $S_{e(av)}$ values, a series of distilled water horizontal infiltration experiments were conducted into a uniform, dry soil. $S_{e(av)}$ was varied by changing the liquid pressure head, h_0, at the inlet to the porous medium. In what follows, the liquids and the material used in the experiments are described, together with the experimental apparatus and the experimental procedures. The results of the experiments are then presented and their interpretation is discussed.

2. Materials and Experimental Procedures

2.1 Liquid and Porous Medium

Distilled water was used for the infiltration experiments; relevant properties for this liquid are given in Table 1.

Table 1: Properties of distilled water at 20°C.

Property	
Dynamic viscosity, μ (g/cm/s)	1.002×10^{-2}
Density, ρ (g/cm^3)	0.998
Surface Tension, σ (dyne/cm)	71.9
Wetting Index in Nevada Sand, $\beta = \cos\phi$[a]	0.53

[a] assumed from the results of Culligan et al. (2005).

All liquid infiltration experiments were conducted using a quartz sand, called Nevada Sand, with an average grain diameter of 0.202 mm and a uniformity coefficient $C_u = D_{60}/D_{10} = 1.9$. To prevent accidental contamination or moistening, the sand was stored in a sealed plastic bucket. Table 2 summarizes the properties of the sand.

Table 2: Properties of Nevada Sand.

Property	
Average particle size, D_{50} (cm)	0.0202
Saturated conductivity, water $K_{s(w)}$ (cm/s)[a]	1.66×10^{-2}

[a] From constant head test (ASTM 2434-68).

2.2 Experimental Apparatus

A schematic of the apparatus used for the horizontal infiltration experiments is shown in Fig. 1.

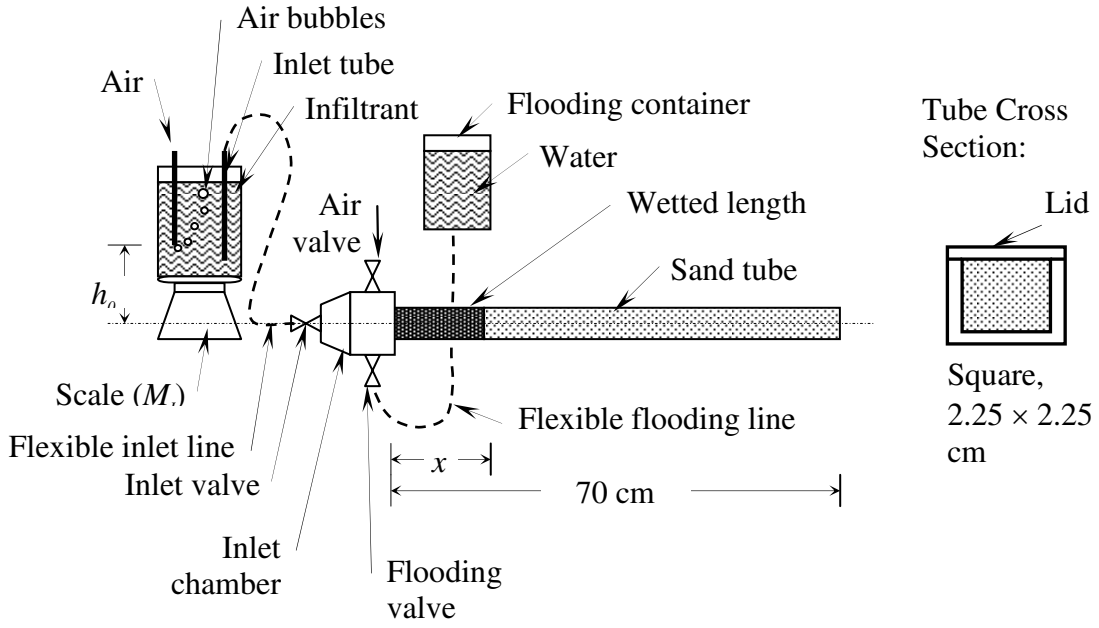

Figure 1: Schematic diagram of experimental apparatus.

The sand was placed in a transparent tube with a square cross-sectional area of internal dimensions of 2.25 × 2.25 cm. The tube was 70 cm in length and annotated by measuring tape marked in 1 mm divisions. The inlet port to a tube consisted of a 3-valve chamber with a brass mesh screen and filter paper system that allowed liquid to enter the tube but

prevented sand loss. Both the mesh screen and filter paper were wetted with distilled water prior to an experiment. A soft tubing line, attached to the inlet valve, connected the chamber to the infiltrant container. The infiltrant container rested on a scale that was used to record the cumulative mass of liquid infiltration into the tube with time, $M_I(t)$. A second container was connected by soft tubing to a base valve in the inlet chamber. This container was used for the initial flooding and final drainage of the chamber. A cap with an opening to atmosphere held the soil in place at the end of each tube while permitting free air drainage. Thus, air was free to escape during all experiments.

2.3 Experimental Procedure

Sand was uniformly deposited in layers into the tube and then vibrated to yield sand specimens with a dry bulk density of 1.64g/cm^3, and a porosity of $n = 0.36$. The apparatus was then assembled and positioned so that it was leveled horizontally and then secured. The infiltrant container was moved relative to the horizontal tube in order to set the desired inlet pressure head, h_0. Next, the infiltrant container was filled with distilled water and placed on the electronic balance. The inlet tube, flexible inlet line and inlet valve were saturated with the water, and then the inlet valve was closed and attached to the inlet chamber. Next, distilled water was placed in the flooding containers, and the flexible flooding line and the flooding valve were saturated. The flooding valve was closed and attached to the inlet container. The top air valve and the flooding valve were opened and the inlet chamber was saturated with liquid. The electronic scale was zeroed. An instant later, the air and flooding valves were closed, the inlet valve was opened and the clock was started. During an experiment, the elapsed time, t, the average front position $x(t)$, and the cumulative infiltration by mass M_I, were recorded. All experiments were conducted at an ambient temperature of approximately 20^{o}C.

Before the liquid front wetted ~90% of the tube, the flooding container was lowered and the inlet valve was closed. The average front position at the mid-height of the tube was read to an accuracy of about 1 mm from the annotated measuring tape. Both the air and the flooding valves were then opened to drain the chamber and terminate the experiment. Depending upon the liquid and the applied inlet pressure head, the duration of the experiments ranged between 20 minutes and ~1.5 hours.

Final water content distributions were obtained at the end of each experiment. Fig. 2 illustrates the employed sampling technique. A set of thin brass pieces (knives), matching the shape of the tube cross-section, was inserted into the sand to partition the tube into sections. Giving preference to sampling closely behind the front, specimens, with dry masses between 5 and 20 g, were acquired. The wet mass of the specimens were determined and then oven dried to enable calculation of the initial gravimetric liquid content, w.

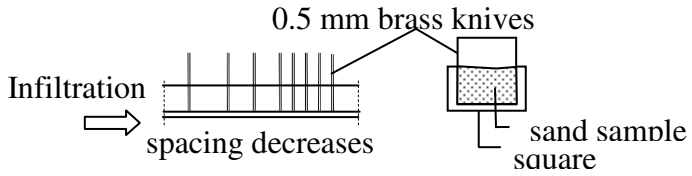

Figure 2: Destructive sampling for liquid content measurements at the end of an experiment.

2.4 Interpretation of Experimental Data

The cumulative infiltration of water per unit area, $i(t)$ was obtained from

$$i(t) = \frac{M_l(t)}{A\rho_l}, \tag{12}$$

where A is the internal cross-sectional area of the tube.

The value of S for each experiment was obtained from a linear regression of $i(t)$ versus $t^{1/2}$ (see Eq. (4)). Fig. 3 depicts one example of the linear $i(t)$ and $x(t)$ vs. $t^{1/2}$ relationship. The observations shown in Fig. 3 were similar to all experiments.

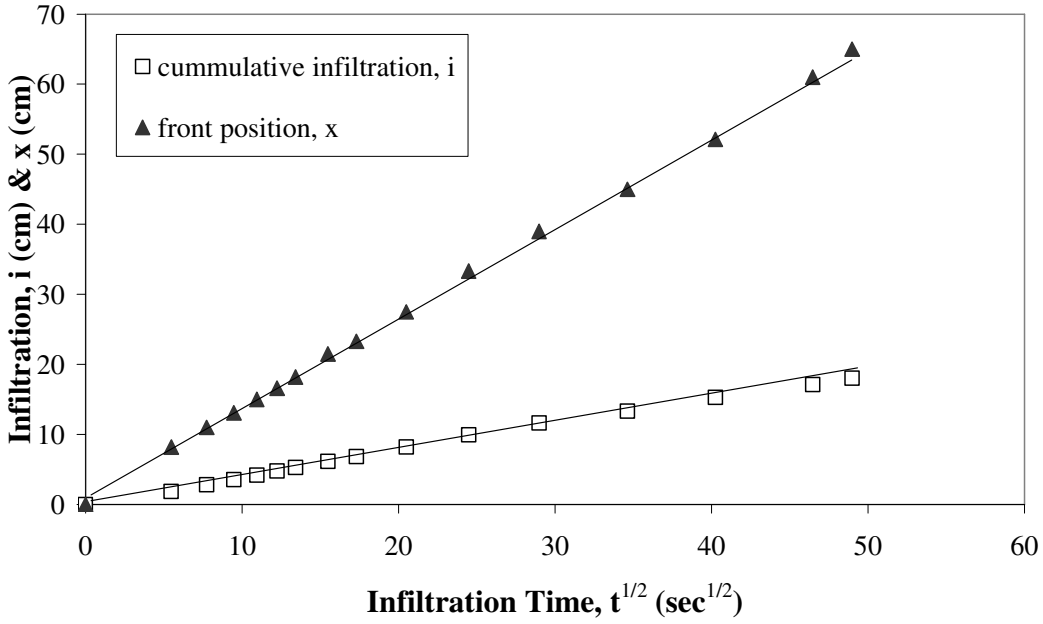

Figure 3: Plot of $i(t)$ versus $t^{1/2}$ for experiment *0.3* at inlet head h_0 = +0 cm (see Table 3).

The average volumetric liquid content of the wetted material in the tube was estimated from $\theta_{av}(t) = i(t)/x(t)$, while the average effective saturation was calculated from $S_{e(av)} = \theta_{av}/n$, where θ_{av} was taken as $\theta_{av}(t)$ at the end of an experiment.

A total of 21 horizontal water infiltration tests were performed. The range of h_0 was –20 cm to +10 cm, giving rise to $S_{e(av)}$ values between 0.64 and 0.86.

3. Discussion of Results

Table 3 presents a summary of results for the water infiltration experiments. Three experiments were performed at each inlet head. The experiments are numbered according to the inlet head and the sequence of the experiment at that inlet head.

Table 3: Summary of water infiltration experiments.

Experiment No.	Porosity n	h_0 cm	θ_{av}	$S_{e(av)}$	S cm/s$^{1/2}$
-20.1	0.36	-20	0.23	0.64	0.2135
-20.2	0.36	-20	0.25	0.69	0.2293
-20.3	0.36	-20	0.23	0.64	0.2284
-15.1	0.36	-15	0.25	0.69	0.2594
-15.2	0.36	-15	0.27	0.75	0.2711
-15.3	0.36	-15	0.26	0.72	0.2688
-10.1	0.36	-10	0.26	0.72	0.3031
-10.2	0.36	-10	0.27	0.75	0.3030
-10.3	0.36	-10	0.24	0.67	0.3109
-5.1	0.36	-5	0.28	0.78	0.3422
-5.2	0.36	-5	0.27	0.75	0.3324
-5.3	0.36	-5	0.26	0.72	0.3146
0.1	0.36	0	0.29	0.81	0.3761
0.2	0.36	0	0.26	0.72	0.3471
0.3	0.36	0	0.29	0.81	0.3740
5.1	0.36	5	0.31	0.72	0.4023
5.2	0.36	5	0.29	0.81	0.4080
5.3	0.36	5	0.30	0.83	0.3954
10.1	0.36	10	0.31	0.86	0.4601
10.2	0.36	10	0.31	0.86	0.4466
10.3	0.36	10	0.31	0.86	0.4744

A log-log scale plot of (S) versus ($S_{e(av)}$) is given in Fig. 4. A theoretical power law of the form $S = A\, S_{e(av)}^{d}$ is included on Fig. 4, where

$$A = \left(\frac{l\beta\sigma n}{\mu} \right)^{1/2} S^{*} \tag{13}$$

and

$$d = -\left(\frac{c-1}{2} \right). \tag{14}$$

As seen in Fig. 4, the relationship between S and $S_{e(av)}$ appears to be well described by a power law, as assumed by the scaling relationships used to derive S^{*} and Φ^{*}. The value of d is 2.355. Hence c = -3.7. The solid line in Fig. 4 is the power law $S = 0.6209\, S_{e(av)}^{2.3551}$ which was obtained using a least squares fit with an R^2=0.93.

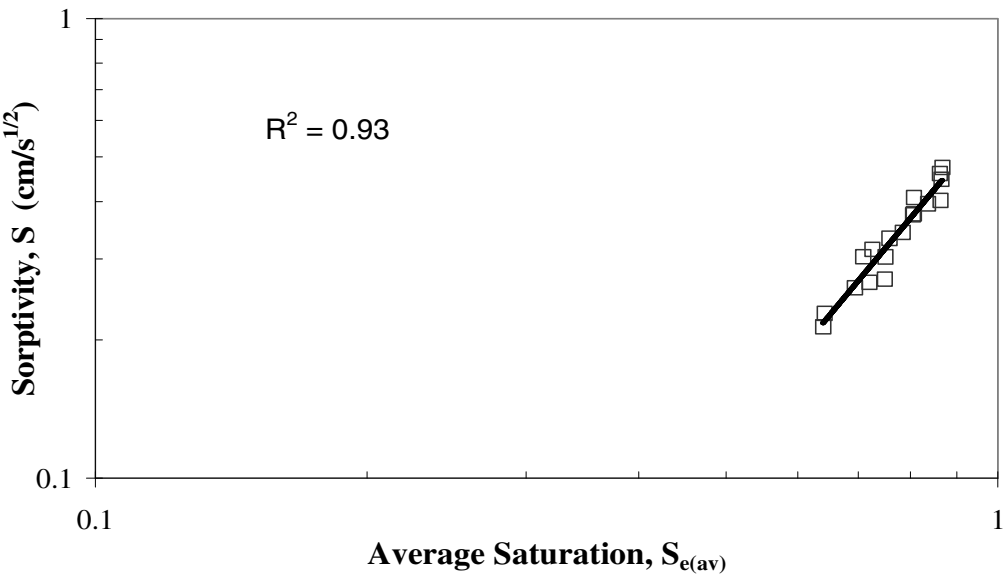

Figure 4: (S) versus ($S_{e(av)}$) in log –log scale.

To quantify the dimensionless sorptivity S_{av}^{*} from Eq. (10) and our measurements of S and $S_{e(av)}$, we adopted the values $\beta = 0.53$ (see Table 1), $l = D_{50}$ (see Table 2) and $n = 0.36$ (see Table 3) giving rise to $S_{av}^{*} = 0.121 \pm .01$. This value compares well with the value of $S_{av}^{*} = 0.128$ that Culligan et al. estimated from the results of their experiments, which were performed using a different set of materials.

Fig. 5 provides a plot of $\theta(x,t_{end})$ versus Φ for selected experiments, where t_{end} is the time at the end of the experiment when the destructive testing method shown in Fig. (2) was used to determine water content as a function of x. As seen, the standard Boltzmann transformation Φ does not lead to a similarity profile for all experimental results. Instead, the trend is for experiments with higher values of $S_{e(av)}$ to lie to the right of those with lower values of $S_{e(av)}$, indicating the important influence of liquid saturation on capillary infiltration.

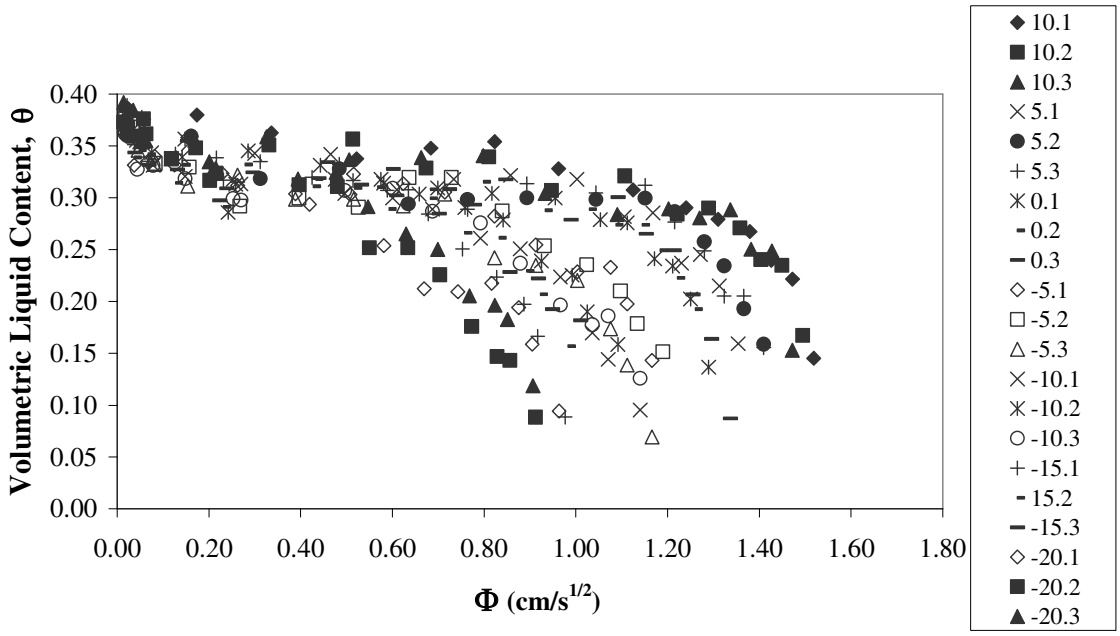

Figure 5: $\theta(x,t_{end})$ versus Φ. Legend values correspond to experiments reported in Table 3.

Fig. 6 is a plot of $\theta^*(x,t_{end})$ versus the proposed *intrinsic* $\Phi_{av}{}^*$ for the same data. $\theta^*(x,t_{end})$ was obtained from Eq. (9) using $\theta_i = 0$ and observed values of θ_m. $\Phi_{av}{}^*$ was calculated using, $\beta_w = 0.53$, $l = D_{50}$ and $c = -3.7$. Excepting the scatter, the profiles of $\theta^*(x,t_{end})$ versus $\Phi_{av}{}^*$ are approximately equivalent for the various liquid pressure heads, providing confidence that the generalized dimensionless Boltzmann variable provides the correct scaling.

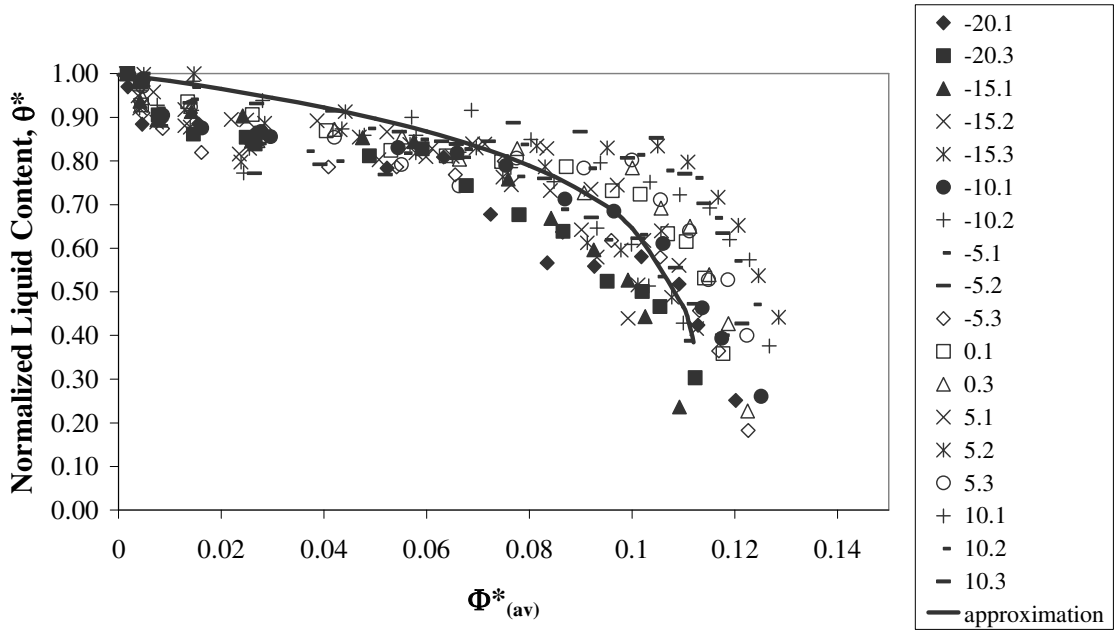

Figure 6: $\theta^*(x,t_{end})$ versus $\Phi_{av}{}^*$. The solid line is the approximation provided by Eq. (16) using $m = 6$ and $s_{av}{}^* = 0.095$. Legend values correspond to experiments reported in Table 3.

An approximation provided by Lockington and Parlange (2003) can also be used to estimate the dimensionless sorptivity S_{av}^* from the similarity profile given in Fig. 6. Taking the dependence of the diffusivity on θ^* to be exponential, such that

$$D(\theta^*) = D_0 e^{m\theta^*}, \tag{15}$$

the normalized wetting profile is given by

$$\theta^*(x) \approx \frac{1}{m}\ln\left[e^m - \frac{m}{D_0^*}\left(\frac{s^*}{2}\Phi^* + \beta^*\Phi^{*2}\right)\right], \tag{16}$$

where

$$D_0^* = \frac{m^2 (s^*)^2}{e^m(2m-1) - m + 1} \tag{17}$$

and

$$\beta^* = \frac{1}{2}\left(\frac{1+m-e^m}{2m(e^m-1)}\right), \tag{18}$$

where s* is the *reduced dimensionless sorptivity* and D_0* is the dimensionless "constant" diffusivity. It is straightforward to show that $s_{av}^* = (\theta_{av}/\theta_m)S_{av}^*$ and $D_{0_{av}}^* = \frac{\mu S_{e_{av}}^c}{l\sigma\beta} D_0$. Note, that the dimensionless "constant" diffusivity changes with the average liquid saturation behind the infiltration front. Thus, it is only a constant for a given $S_{e(av)}$.

Eq. (16) has been fit to the profile given on Fig. (6) using $m = 6$ and $s_{av}^* = 0.095$. Culligan et al. (2005) reported values of $m = 6$ and $s_{av}^* = 0.105$ from the interpretation of their experiments. Again, the good agreement between the values estimated from the experiments reported here and those reported by Culligan et al. (2005) provides confidence in the existence of the proposed dimensionless sorptiviy and the dimensionless Boltzmann transformation. Knowing S_{av}^* (or s_{av}^*) Eq. (10) can, theoretically, be used to calculate the sorptivity S, for a wide range of conditions. Furthermore, Eq. (11) can be used to estimate values of θ at any time t, or location x, in a horizontal soil domain experiencing liquid infiltration.

4. Conclusions

The dependence of sorptivity on $S_{e(av)}$ for infiltration into dry material was investigated in a series of twenty-one distilled water horizontal infiltration experiments that were conducted in a uniform, dry sand packed at an average porosity $n = 0.36$. $S_{e(av)}$ was altered by varying h_0, the liquid pressure head at the inlet to the porous medium. h_0 values between –20 cm and +10 cm gave rise to $S_{e(av)}$ values between 0.64 and 0.86. The results of the experiments show that sorptivity $\propto S_{e(av)}^{3.2}$, confirming that a power law relationship between sorptivity and $S_{e(av)}$ is appropriate for the soil conditions tested here.

The experimental results were used to examine the validity of the dimensionless S^*, and accompanying dimensionless Boltzmann transformation Φ^*, proposed by Culligan et al. (2005). The magnitude of the dimensionless sorptivity, based on θ_{av}, was calculated from experimental results assuming, $\beta = 0.53$, $l = D_{50}$ and $n = 0.36$, giving rise to $S_{av}^* = 0.121$, which is close to the value of $S_{av}^* = 0.128$ proposed by Culligan et al. Liquid content profiles from the infiltration experiments were used to examine the validity of the dimensionless Boltzmann variable. The liquid content profiles were obtained from

destructive sampling of a soil tube at the end of experiment. Excepting some scatter, the profiles of normalized liquid content versus Φ_{av}^{*} were approximately equivalent, indicating that the dimensionless Boltzmann variable can be used to generate a similarity profile for moisture content, even when infiltration takes place under different degrees of liquid saturation.

The concept of an intrinsic sorptivity is powerful. If it can be demonstrated that Miller-similar materials share a defined value of S^{*}, then the scaling relationship provided in Eq. (10) of this paper can be used to calculate the sorptivity S for a wide range of conditions, and thereby capillary driven liquid infiltration under a wide range of conditions.

Acknowledgements

The work was supported, in part, by Dr. Culligan's and Dr. Germaine's Collaborative National Science Foundation Grant CMS-04-09521. The authors appreciate Mr. Stephen Rudolph's assistance with the fabrication of the equipment.

References Cited

Barry, D.A., Parlange, J.-Y., Haverkamp, R., Ross, P. J. (1995). "Infiltration under ponded conditions: 4. An explicit predictive infiltration formula." *Soil Sci.,* 160: 8-17. 1995.

Culligan, P. J., Ivanov, V., Germaine, J. T. (2005). "Sorptivity and liquid infiltration into dry soil". *Advances in Water Resources 28.,* 1010-1020.

Green, W. H., Ampt, G.A. (1911). "Studies on soil physics, Part I. Flow of air and water through soils". *J. Ag. Sci.*, 4:1-24.

Lockington, D., Parlange, J.-Y., Dux, P. (1999). "Sorptivity and the estimation of water penetration into unsaturated concrete". *Materials and Structures*., Vol. 32, 342-347.

Lockington, D., Parlange, J.-Y. (2003). "Anomalous water absorption in porous materials". *J. Phys. D: Appl. Phys*., 36, 760-767.

Miller, E. E. (1980). *Similitude and scaling of soil-water phenomena, in Applications of Soil Physics, edited by D- Hillel, 300 – 318*, Academic, San Diego, California.

Neilson, D.R., Biggar, J. W., Davidson, J. M. (1962). "Experimental consideration of diffusion analysis in unsaturated flow problems". *Soil Sci. Soc. Am Proc.* 26:107-11.

Parlange, J.-Y., Lise, I., Braddock, R.D. and Smith, R.E. (1982). "The three parameter infiltration equation." *Soil Sci.*, 133(6): 337-341.

Slichter, C. S. (1898) "Theoretical investigation of the motion of groundwaters. Nineteenth Annual Rep., Pt. 2:295-384." Washington D.C: US Geological Survey.

Smith, R.E., Parlange, J.-Y. (1978). "A parameter-efficient hydrological infiltration model". *Water Resour. Res.,* 14(3): 533-38.

Tindall, J.A., Kunkel, J. R. (1999). *Unsaturated zone hydrology for scientists and engineers.* Prentice-Hall, Englewood Cliffs, N.J.